EXCLI Journal 2021;20:907-921 – ISSN 1611-2156
Received: February 27, 2021, accepted: May 10, 2021, published: May 18, 2021

Original article:

NOVEL 1,2,4-OXADIAZOLE DERIVATIVES AS SELECTIVE BUTYRYLCHOLINESTERASE INHIBITORS: DESIGN, SYNTHESIS, AND BIOLOGICAL EVALUATION

Maryam Nazari[a], Elham Rezaee[a,*], Roshanak Hariri[b], Tahmineh Akbarzadeh[b], Sayyed Abbas Tabatabai[a,*]

[a] Department of Pharmaceutical Chemistry, School of Pharmacy, Shahid Beheshti University of Medical Sciences, Tehran, Iran
[b] Department of Medicinal Chemistry, Faculty of Pharmacy, Tehran University of Medical Sciences, Tehran, Iran

* **Corresponding authors:** Sayyed Abbas Tabatabai and Elham Rezaee, Department of Pharmaceutical Chemistry, School of Pharmacy, Shahid Beheshti University of Medical Sciences, Tehran, Iran. No. 2660, Vali-e-Asr., Tehran 1991953381, Iran, Tel: 00982188200093; Fax: 00982188665341;
E-mails: sa_tabatabai@sbmu.ac.ir (Sayyed Abbas Tabatabai); e.rezaee63@sbmu.ac.ir (Elham Rezaee)

http://dx.doi.org/10.17179/excli2021-3569

GRAPHICAL ABSTRACT

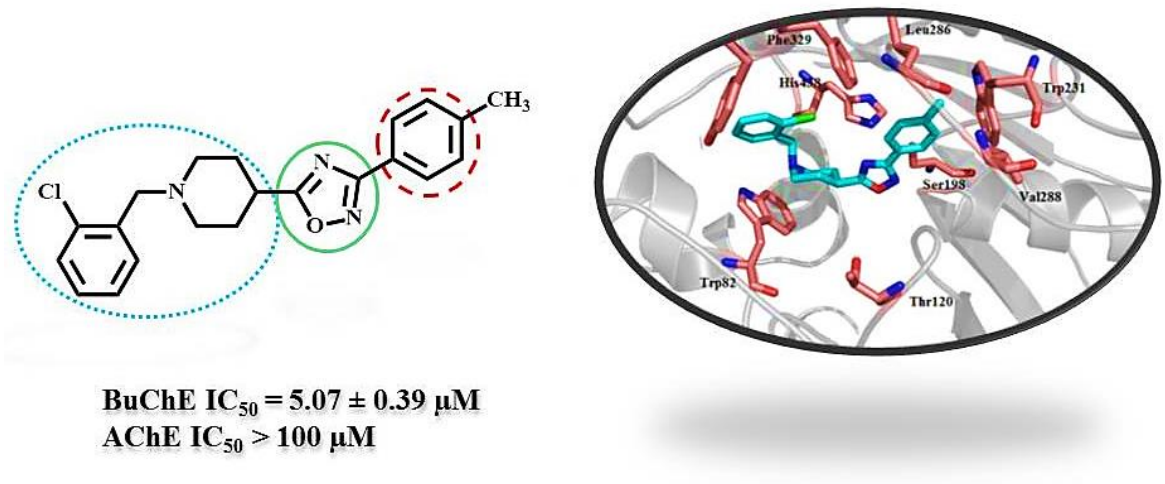

Figure 1: *N*-benzylpiperidine-based derivatives of 1,2,4-oxadiazole as novel selective inhibitors of butyrylcholinesterase enzyme

ABSTRACT

Alzheimer's disease (AD) is a progressive mental disorder that brings a huge economic burden to the healthcare systems. During this illness, acetylcholine levels in the cholinergic systems gradually diminish, which results in severe memory loss and cognitive impairments. Moreover, Butyrylcholinesterase (BuChE) enzyme participates in

EXCLI Journal 2021;20:907-921 – ISSN 1611-2156
Received: February 27, 2021, accepted: May 10, 2021, published: May 18, 2021

cholinergic neurotransmission regulation by playing a prominent role in the latter phase of AD. In this study, based on donepezil, which is an effective acetylcholinesterase (AChE) inhibitor, a series of 1,2,4-oxadiazole compounds were designed, synthesized and their inhibitory activities towards AChE and BuChE enzymes were evaluated. Some structures exhibited a higher selectivity rate towards BuChE in comparison to donepezil. Notably, compound **6n** with an IC_{50} value of 5.07 µM and an SI ratio greater than 19.72 showed the highest potency and selectivity towards BuChE enzyme. The docking result revealed that compound **6n** properly fitted the active site pocket of BuChE enzyme, and formed desirable lipophilic interactions and hydrogen bonds. Moreover, according to *in silico* ADME studies, these compounds have proper potential for being developed as new oral anti-Alzheimer's agents.

Keywords: Alzheimer's disease, 1,2,4-oxadiazole, biological evaluation, butyrylcholinesterase inhibitor, synthesis

1 INTRODUCTION

Alzheimer's disease (AD) is a progressive illness characterized by loss of memory, the reduced thinking and cognition abilities, psychiatric disorders like depression, and difficulties in performing daily activities (Sugimoto et al., 2012; Alzheimer's Association, 2013; Soria Lopez et al., 2019; Sengoku, 2020). According to the World Alzheimer's Report in 2019, 50 million people suffer from dementia worldwide, and this number is estimated to increase up to more than 152 million by 2050 (Alzheimer's Disease International 2019). Accordingly, this fatal multifactorial disease is very burdensome due to its illness duration before death (Alzheimer's Association 2017; Cass 2017; Femminella et al., 2018). The complex pathological hallmarks of AD seem to result from chronic oxidative stress, mitochondrial dysfunction, extracellular beta-amyloid (Aβ) production, and intraneuronal neurofibrillary tau tangles accumulation (Oboudiyat et al., 2013; Anand et al., 2014; Busche and Hyman, 2020; Vaz and Silvestre, 2020). In addition, AD is accompanied with the deterioration of the cholinergic system (Hampel et al., 2018; Sharma, 2019). Acetylcholine (ACh) is one of the substantial neurotransmitters in particular brain synapses, deficiency of which would lead to cognitive impairment of the disease (Amenta and Tayebati, 2008; Richter et al., 2018; Hampel et al., 2019). There are two main cholinesterase enzymes (ChEs) throughout the body belonging to the α/β-hydrolase family, which were found to be responsible for the regulation of cholinergic neurotransmission. Acetylcholinesterase (AChE) is mostly found in neuronal cells, the primary function of which is the degradation of ACh. While butyrylcholinesterase (BuChE), also named as nonspecific or pseudocholinesterase, is mainly produced by glial cells, so it is liable for the hydrolysis of choline-based esters (Franjesevic et al., 2019). The structures of both ChEs were found to be very similar as ChEs sequence comparison exhibited a similarity of 66 % (Sawatzky et al., 2016). In this regard, the AChE enzyme has a greater tendency to small molecules like ACh, but BuChE provides a wider space for larger substrates (Franjesevic et al., 2019).

Based on the prominent role of BuChE at the late stages of AD pathogenesis (Darvesh et al., 2003), and small side effects of BuChE inhibitors, targeting BuChE might be a promising strategy for the control of disease progression. Therefore, recent attempts have been made to design selective BuChE inhibitors (Figure 2) (Li et al., 2017). As shown in Figure 2, compound **1** is a carbamate-based derivative and compound **2** is a non-cytotoxic benzamide with a high selectivity and inhibitory activity towards BuChE enzyme (Wajid et al., 2019; Wu et al., 2019). Compounds **3** and **4**, which were designed based on donepezil and tacrine, demonstrated a high selectivity against BuChE enzyme, respectively (de Andrade et al., 2019; Joubert and Kapp, 2020). Furthermore, previous oxadia-

EXCLI Journal 2021;20:907-921 – ISSN 1611-2156
Received: February 27, 2021, accepted: May 10, 2021, published: May 18, 2021

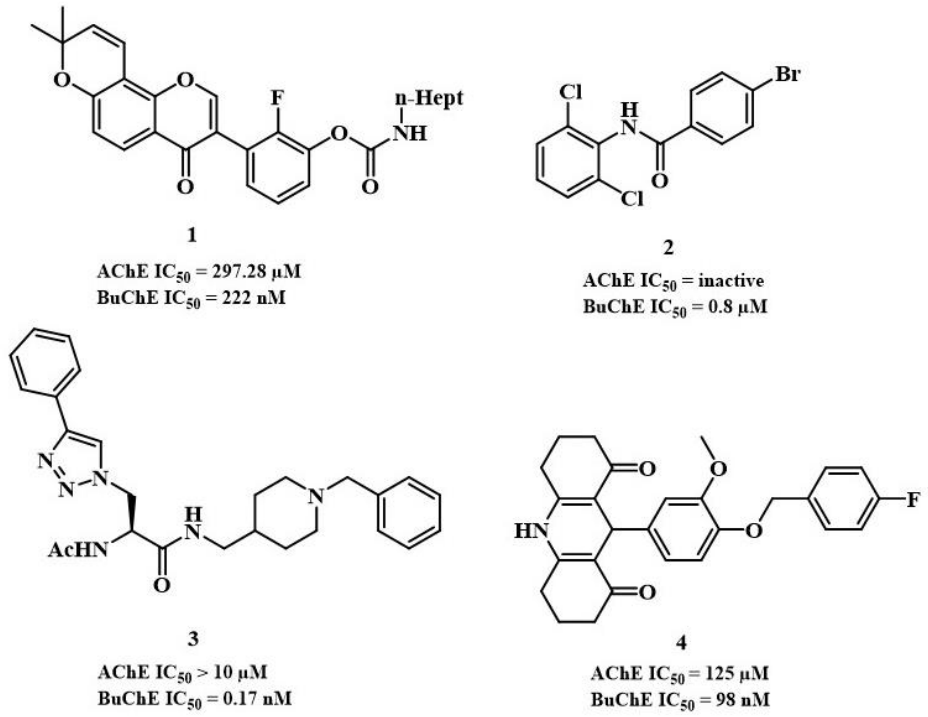

Figure 2: Chemical structures of highly selective BuChE inhibitors

zole derivatives synthesized as the selective BuChE showed no significant inhibitory activity and selectivity against this enzyme (Zhang et al., 2019).

Donepezil, a selective AChE inhibitor with a low anti-BuChE effect, is currently administered as an anti-AD medication due to possessing fewer side effects and longer half-life. Moreover, it has been considered as an appealing lead compound for designing new agents (van Greunen et al., 2017). However, this medicine could only relieve the symptoms of the disease, and it is incapable of being effective on moderate to severe AD (Coman and Nemeş, 2017). Accordingly, the starting point of our investigation was donepezil in order to design a structure with the improved inhibitory effects on BuChE that might be promising in the latter phase of the disease. Therefore, we designed the novel donepezil-like compounds by maintaining the *N*-benzylpiperidine moiety and replacing the indanone segment with a 1,2,4-oxadiazole ring that was connected to an aromatic ring with different substituents (Figure 3). In the current study, synthesis, biological evaluation, docking study, and ADME prediction were reported.

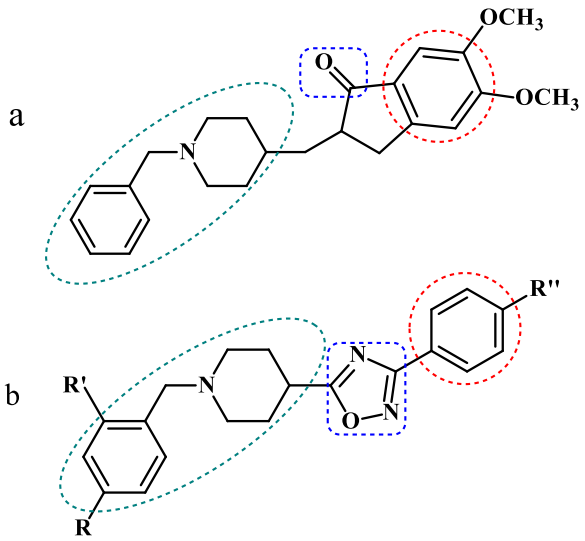

Figure 3: The corresponding parts of donepezil (**a**) to the designed compounds (**b**) are shown.

EXCLI Journal 2021;20:907-921 – ISSN 1611-2156
Received: February 27, 2021, accepted: May 10, 2021, published: May 18, 2021

2 RESULT AND DISCUSSION

2.1 Chemistry

According to Figure 4, the commercially available starting material **1** and para- or ortho-substituted benzyl bromides **2** were mixed for 48 hours in the presence of potassium carbonate in order to afford various N-benzylated intermediate **3**. A mixture containing benzonitrile **4**, hydroxylamine hydrochloride and sodium carbonate in ethanol/H_2O was refluxed for 24 hours to achieve para-substituted amidoximes **5**. The 1, 2, 4-oxadiazole ring was closed by the reaction of intermediate **3** with several amidoximes **5** in the presence of sodium ethoxide. Finally, by the addition of hydrochloric acid in diethyl ether, compounds **6a-6t** were achieved (Zavareh et al., 2014).

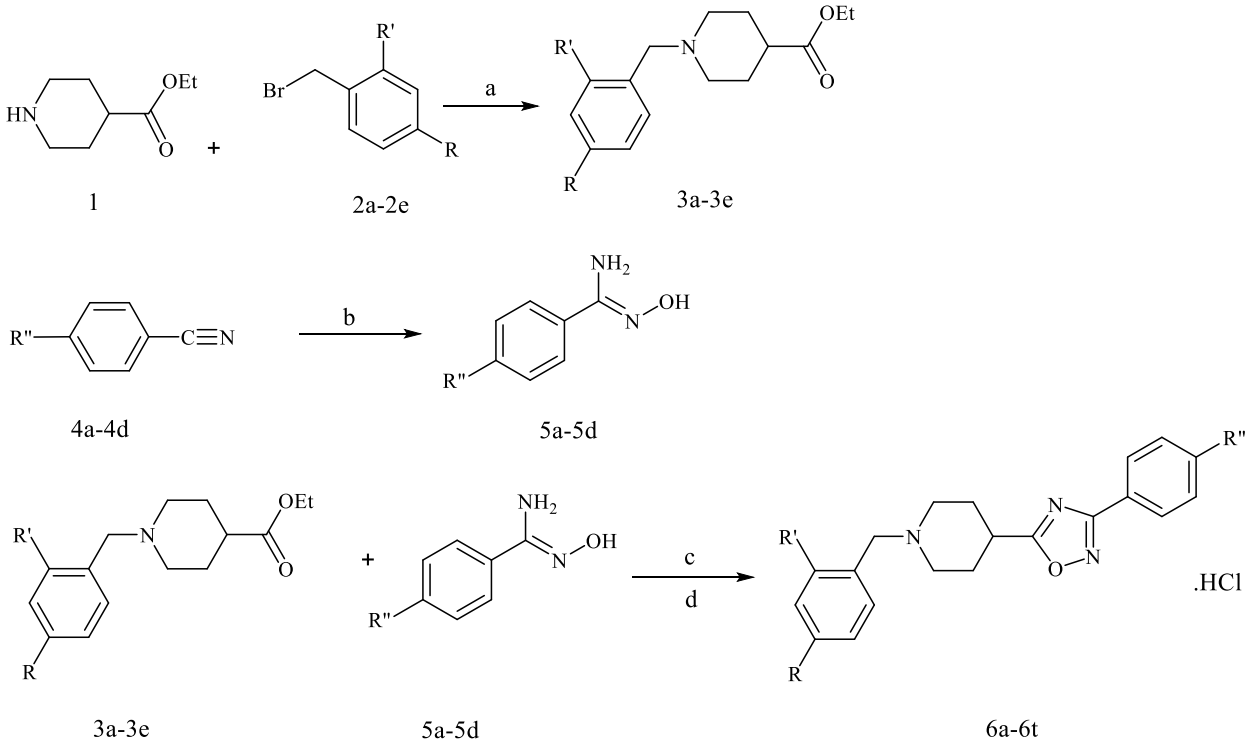

6a, R = H, R' = H, R" = H

6b, R = H, R' = H, R" = CH_3

6c, R = H, R' = H, R" = Cl

6d, R =H, R' = H, R" = F

6e, R = F, R' = H, R" = H

6f, R = F, R' = H, R" = CH_3

6g, R = F, R' = H, R" = Cl

6h, R = F, R' = H, R" = F

6i, R = Cl, R' = H, R" = H

6j, R = Cl, R' = H, R" = CH_3

6k, R = Cl, R' = H, R" = Cl

6l, R = Cl, R' = H, R" = F

6m, R = H, R' =Cl, R" = H

6n, R = H, R' =Cl, R" = CH_3

6o, R = H, R' =Cl, R" = Cl

6p, R = H, R' =Cl, R" = F

6q, R = CH_3, R' = H, R" = H

6r, R = CH_3, R' = H, R" = CH_3

6s, R = CH_3, R' = H, R" = Cl

6t, R = CH_3, R' = H, R" = F

Figure 4: Reagents and conditions: (a) K_2CO_3, DMF, r.t, 48 h, stir, 59.7 %-76.6 %; (b) Hydroxylammonium chloride, Na_2CO_3, H_2O, EtOH, 24 h, reflux, 68.2 %-96.5 %; (c) NaOEt, dry EtOH, 24 h, reflux, (d) HCl in diethyl ether, 20.9 %-56.3 %.

EXCLI Journal 2021;20:907-921 – ISSN 1611-2156
Received: February 27, 2021, accepted: May 10, 2021, published: May 18, 2021

2.2 Inhibitory activity against AChE and BuChE enzymes

The inhibitory activity of the designed compounds against BuChE and AChE was evaluated using Ellman's method. During this process, donepezil was considered as a standard compound. As summarized in Table **1**, some compounds in this series depicted proper inhibitory activities against BuChE with desirable IC_{50} values (5.07 µM to 81.16 µM), and also exhibited more selectivity towards BuChE, rather than AChE, in comparison with donepezil. Additionally, compounds **6n** and **6b** with a methyl group in the R″ position were found to be the most potent ones for BuChE with IC_{50} values of 5.07 µM and 9.81 µM and high selectivity with SI ratios greater than 19.72 and 10.19, respectively. However, compound **6a** with no substituent in this position showed moderate potency against BuChE (IC_{50}= 14.23 µM) and AChE (IC_{50}= 35.46 µM).

Apparently, substitution in the R and R′ positions would enhance inhibitory potency in the order of 2-chloro > 4-chloro > 4-fluoro, respectively, indicating that the large lipophilic electron-withdrawing groups in these places would be in favor of the anti-BuChE activity.

Table 1: Inhibitory activities of the 1,2,4-oxadiazole derivatives **(6a-t)**

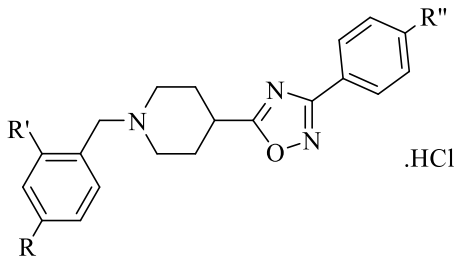

Compound	R	R'	R"	AChE[a] IC_{50} (µM) ± SD	BuChE[a] IC_{50}(µM) ± SD	SI[b]
6a	H	H	H	35.46 ± 0.66	14.23 ± 0.39	2.49
6b	H	H	CH_3	>100	9.81 ± 0.016	>10.19
6c	H	H	Cl	>100	>100	NA[c]
6d	H	H	F	21.16 ± 0.13	24.84 ± 0.97	0.85
6e	F	H	H	>100	>100	NA[c]
6f	F	H	CH_3	>100	50.70 ± 0.06	>1.97
6g	F	H	Cl	>100	>100	NA[c]
6h	F	H	F	>100	>100	NA[c]
6i	Cl	H	H	>100	>100	NA[c]
6j	Cl	H	CH_3	>100	50.35 ± 0.77	>1.98
6k	Cl	H	Cl	>100	>100	NA[c]
6l	Cl	H	F	>100	>100	NA[c]
6m	H	Cl	H	>100	>100	NA[c]
6n	H	Cl	CH_3	>100	5.07 ± 0.39	>19.72
6o	H	Cl	Cl	>100	81.16 ± 0.98	>1.23
6p	H	Cl	F	>100	>100	NA[c]
6q	CH_3	H	H	>100	>100	NA[c]
6r	CH_3	H	CH_3	>100	62.83 ± 0.65	>1.59
6s	CH_3	H	Cl	>100	>100	NA[c]
6t	CH_3	H	F	>100	>100	NA[c]
Donepezil	-	-	-	0.079 ± 0.002	5.19± 0.38	0.015

[a] Inhibition activities were measured using Ellman's method. IC_{50} values represent the inhibitory concentrations required to decrease enzyme activity by 50 % and expressed as mean ± SD.
[b] Selectivity Index which is determined as ratio AChE IC_{50}/BuChE IC_{50}. [c] Not applicable

EXCLI Journal 2021;20:907-921 – ISSN 1611-2156
Received: February 27, 2021, accepted: May 10, 2021, published: May 18, 2021

2.3 Docking study

The molecular docking study was conducted using AutoDock Tools software version 1.5.6rc3. In this regard, the X-ray crystallographic structure of the human BuChE (PDB Code 1P0I) was utilized as an enzyme structure. The docked binding mode was analyzed for the interactions between compound **6n** and BuChE. As shown in Figure 5**,** the compound **6n** was well accommodated inside the gorge active site and adopted a U-shaped conformation. A hydrogen bond was also observed between the nitrogen of the pyridine ring and Trp82. The 4-methyl phenyl moiety of **6n** was located in the enzyme's acyl pocket via forming lipophilic interactions with residues of Leu286, Trp231, and Val288. Subsequently, the 1,2,4-oxadiazole ring could form hydrogen bonds with His438, Ser198, and Thr120. Moreover, the benzyl ring might have lipophilic interactions with Phe329, Trp 82 and Tyr332.

2.4 ADME properties

To predict the *in silico* ADME features of our proposed novel compounds, an online Swissadme calculator was used. According to Table **2**, all the structures abided by the Lipinski's rule of five criteria (Ertl et al., 2000), and the percentage absorption (%ABS) was predicted at 94.45 %. Accordingly, it seems that, these compounds might be orally bioavailable agents, which is known as a favorable route of drug administration.

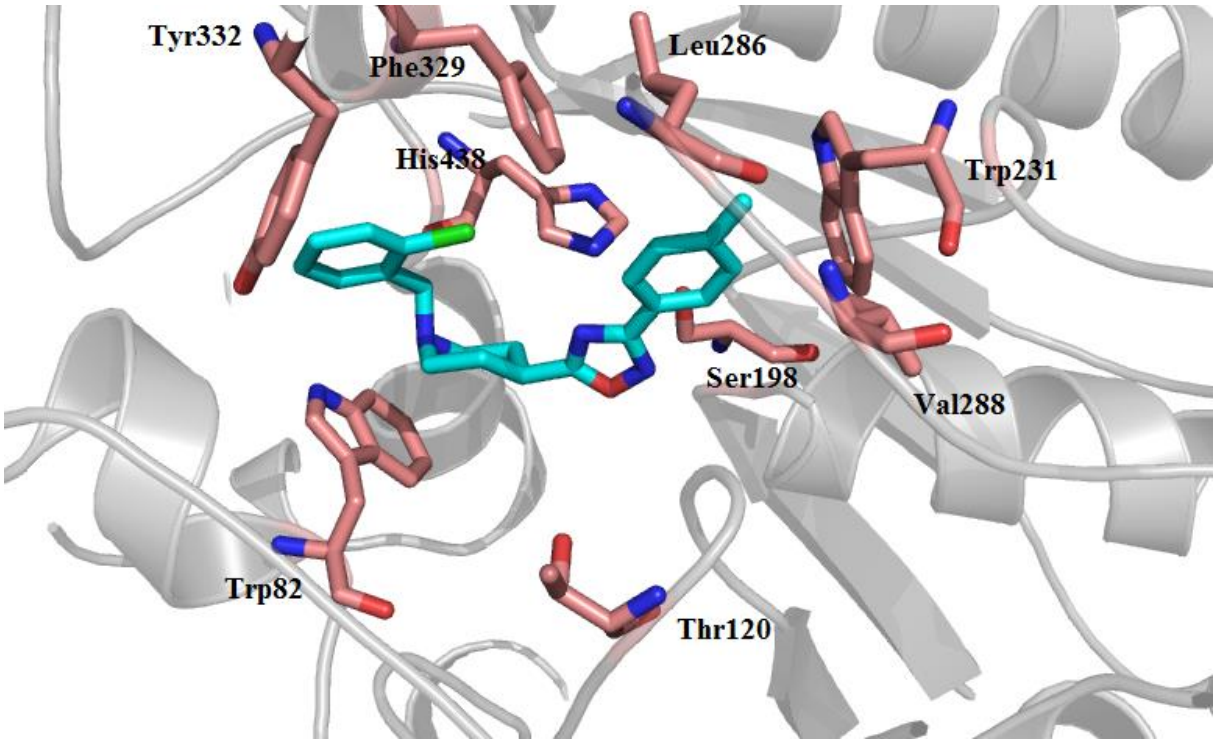

Figure 5: Compound **6n** (light blue sticks) in the catalytic pocket of BuChE (PDB: 1P0I). A hydrogen bond was observed between nitrogen of the pyridine ring and Trp82. The 4-methyl benzene moiety of **6n** was located in the acyl pocket of the enzyme via lipophilic interactions.
Hydrogen bonds could form between oxadiazole ring with His438, Ser198 and Thr120. Moreover, the benzyl ring had hydrophobic interactions with Phe329 and Tyr332.

EXCLI Journal 2021;20:907-921 – ISSN 1611-2156
Received: February 27, 2021, accepted: May 10, 2021, published: May 18, 2021

Table 2: Pharmacokinetic parameters important for oral bioavailability of the synthesized compounds (**6a-t**)

Compound	%ABS	TPSA (A^2)	*n*-ROTB	MW	mLog*P*	*n*-ON acceptors	*n*-OHNH donors	Lipinski's violations
6a	94.45	42.16	4	319.40	3.03	4	0	0
6b	94.45	42.16	4	333.43	3.66	4	0	0
6c	94.45	42.16	4	353.85	3.92	4	0	0
6d	94.45	42.16	4	337.39	3.81	5	0	0
6e	94.45	42.16	4	337.39	3.41	5	0	0
6f	94.45	42.16	4	351.42	4.03	5	0	0
6g	94.45	42.16	4	371.84	3.90	5	0	0
6h	94.45	42.16	4	355.38	3.79	6	0	0
6i	94.45	42.16	4	353.85	3.52	4	0	0
6j	94.45	42.16	4	367.87	4.14	4	0	0
6k	94.45	42.16	4	388.29	4.00	4	0	0
6l	94.45	42.16	4	371.84	4.30	5	0	0
6m	94.45	42.16	4	353.85	3.52	4	0	0
6n	94.45	42.16	4	367.87	4.14	4	0	0
6o	94.45	42.16	4	388.29	4.41	4	0	0
6p	94.45	42.16	4	371.84	4.30	5	0	0
6q	94.45	42.16	4	333.43	3.25	4	0	0
6r	94.45	42.16	4	375.45	3.47	4	0	0
6s	94.45	42.16	4	367.87	3.74	4	0	0
6t	94.45	42.16	4	351.42	3.63	5	0	0
Donepezil	95.62	38.77	6	381.51	2.60	4	0	0

%ABS: percentage absorption; TPSA: topological polar surface area; *n*-ROTB: number of rotatable bonds; MW: molecular weight; mLog *P*: logarithm of partition coefficient of the compound between n-octanol and water; *n*-ON acceptors: number of hydrogen bond acceptors; *n*-OHNH donors: number of hydrogen bonds donors

3 CONCLUSION

In this study, a series of 1,2,4-oxadiazole derivatives, as novel selective inhibitors of BuChE, were rationally designed and synthesized. Thereafter, the inhibitory activities of the compounds against AChE and BuChE enzymes were evaluated. Based on our findings, some compounds exhibited high selectivity towards BuChE and the most potent compound was found to be **6n** (IC_{50} = 5.07 µM, SI ratio > 19.72) with chlorine and methyl group in R′ and R″ positions, respectively. This compound possessed an appropriate lipophilicity as well as hydrophobic interactions with the active site of the BuChE. Indeed, it seems that the presence of the methyl group in the R″ position promoted this selectivity. Additionally, *in silico* ADME prediction showed the exemplary oral bioavailability of these structures. In summary, the designed structures have the potential to act as promising starting points in order to develop more selective BuChE inhibitors with the improved pharmacokinetic properties for the treatment of Alzheimer's disease.

4 EXPERIMENTAL SECTION

4.1 Chemistry

All the reagents used in this study were achieved from Aldrich or Merck Company with no further purification. ^{1}H NMR and ^{13}C NMR spectra were afforded by a Bruker Avance II spectrophotometer using $CDCl_3$, as a solvent, and tetramethylsilane, as an internal standard, at 400.20 and 100.64 MHz, respectively. Chemical shifts were reported in parts per millions (ppm). All mass spectra were obtained using HPLC Agilent 1100 spectrometer. Melting points were also taken using an Electrothermal 9100 apparatus and were not

corrected afterward. A Perkin Elmer 834 spectrometer was utilized to record infrared spectra and the absorptions were expressed on the wave number (cm^{-1}) scale ranged from 400 to 4000 cm^{-1}.

4.1.1 General procedure for the synthesis of ethyl 1-benzylpiperidine-4-carboxylate derivatives (3a-e)

Ethyl piperidine-4-carboxylate **1** (1 equiv) was dissolved in 15 ml DMF and the mixture was then placed in a round bottom flask followed by the addition of K_2CO_3 (2 equiv) under stirring condition. Suitable benzyl bromide **2a-d** (1 equiv) was added dropwise while the flask was cooled in an ice bath. Thereafter, the ice bath was removed, and the mixture was stirred for 48 h at room temperature. Afterward, the medium was filtered, and the filtrate was extracted with water and diethyl ether. Finally, the organic layer was dried over $MgSO_4$ and evaporated in vacuum in order to afford yellow oily liquid.

4.1.1.1 ethyl 1-benzylpiperidine-4-carboxylate (3a)

Yellow oily liquid; yield: 59.7 %; IR (KBr, cm^{-1}): 1733 (C=O); LC-MS $[M + 1]^+$: m/z 248.

4.1.1.2 ethyl 1-(4-fluorobenzyl)piperidine-4-carboxylate (3b)

Yellow oily liquid; yield: 73.5 %; IR (KBr, cm^{-1}): 1732 (C=O); LC-MS $[M + 1]^+$: m/z 265.9.

4.1.1.3 ethyl 1-(4-chlorobenzyl)piperidine-4-carboxylate (3c)

Yellow oily liquid; yield: 68.9 %; IR (KBr, cm^{-1}): 1738 (C=O); LC-MS $[M + 1]^+$: m/z 281.9.

4.1.1.4 ethyl 1-(2-chlorobenzyl)piperidine-4-carboxylate (3d)

Yellow oily liquid; yield: 60.6 %; IR (KBr, cm^{-1}): 1738 (C=O); LC-MS $[M + 1]^+$: m/z 282.

4.1.1.5 ethyl 1-(4-methylbenzyl)piperidine-4-carboxylate (3e)

Yellow oily liquid; yield: 76.6%; IR (KBr, cm^{-1}): 1733 (C=O); LC-MS $[M + 1]^+$: m/z 262.

4.1.2 General procedure for the synthesis of N′-hydroxybenzamidine derivatives (5a-d)

A solution of hydroxylamonium chloride (2 equiv) and sodium carbonate (1 equiv) dissolved in 15 ml H_2O was added to a mixture of a nitrile **4** (1 equiv) dissolved in 15 ml ethanol 96 %, which were then heated under reflux. After 24 h, the mixture was extracted with diethyl ether and concentrated in vacuum. Finally, the light yellow powder was achieved with no purification.

4.1.2.1 N′-hydroxybenzamidine (5a)

Light yellow powder; yield: 96.5 %; mp: 68-70 °C; IR (KBr, cm^{-1}): 1657 (C=N), 3349, 3468 (NH_2); LC-MS $[M + 1]^+$: m/z 136.9.

4.1.2.2 N′-hydroxy-4-methylbenzamidine (5b)

Light yellow powder; yield: 81.9 %; mp: 145.8-148 °C; IR (KBr, cm^{-1}): 1661 (C=N), 3365, 3493 (NH_2); LC-MS $[M + 1]^+$: m/z 150.9.

4.1.2.3 4-chloro-N′-hydroxy benzamidine (5c)

Light yellow powder; yield: 87.5 %; mp: 125.8-128 °C; IR (KBr, cm^{-1}): 1655 (C=N), 3337, 3462 (NH_2); LC-MS $[M + 1]^+$: m/z 170.8.

4.1.2.4 4-fluoro-N′-hydroxy benzamidine (5d)

Light yellow powder; yield: 68.2 %; mp: 94.5-99.5 °C; IR (KBr, cm^{-1}): 1653 (C=N), 3363, 3457 (NH_2); LC-MS $[M + 1]^+$: m/z 154.9.

4.1.3 General procedure for the synthesis of 1,2,4-oxadiazole derivatives (6a-t)

A suitable *N*-benzylated ester **3a-e** (5 equiv) was dissolved in 15 ml super dry ethanol and stirred under reflux. Subsequently, proper amidoxime **5a-d** (1 equiv) and ethanolic solution of sodium ethoxide 20 % (5 equiv) were added to the obtained mixture. After one day, the mixture was concentrated in vacuum, and the precipitate was washed with *n*-hexane. The *n*-hexane layer was collected and then concentrated under the reduced pressure. Accordingly, the obtained powder was recrystallized from $EtOH/H_2O$.

The hydrochloride salt of the final product was achieved by the addition of 3 equiv HCl in diethyl ether.

4.1.3.1 5-(1-benzylpiperidin-4-yl)-3-phenyl-1,2,4-oxadiazole (6a)

Light yellow powder; yield: 54.4 %; mp: 70.8-71.2 °C; IR (KBr, cm^{-1}): 1587 (C=N), 1142 (C-O); LC-MS $[M + 1]^+$: m/z 320; ^1H NMR ($CDCl_3$, 400 MHz) δ: 2.02-2.20 (m, 6H, H-piperidine), 2.94-3.03 (m, 3H, H-piperidine), 3.54 (s, 2H, CH_2-benzyl), 7.25-7.34 (m, 5H, H_2, H_3, H_4, H_5, H_6-benzyl), 7.47-7.48 (m, 3H, H_3, H_4, H_5-phenyl), 8.07-8.08 (m, 2H, H_2, H_6-phenyl); ^{13}C NMR ($CDCl_3$, 100 MHz) δ: 29.56 ($2CH_2$), 34.64 (CH), 52.75 ($2CH_2$), 63.20 (CH_2), 126.99 (C), 127.07 (CH), 127.42 (2CH), 128.25 (2CH), 128.80 (2CH), 129.04 (2CH), 131.05 (CH), 138.29 (C), 168.19 (C), 182.07 (C); Anal. calcd for $C_{20}H_{21}N_3O$: C, 75.21; H, 6.63; N, 13.16, found: C, 75.43; H, 6.61; N, 13.13.

4.1.3.2 5-(1-benzylpiperidin-4-yl)-3-(p-tolyl)-1,2,4-oxadiazole (6b)

Light yellow powder; yield: 32.9 %; mp: 88.5-89.8 °C; IR (KBr, cm^{-1}): 1582 (C=N), 1145 (C-O), 1346,1440 (CH_3); LC-MS $[M + 1]^+$: m/z 333.9; ^1H NMR ($CDCl_3$, 400 MHz) δ: 2.00-2.18 (m, 6H, H-piperidine), 2.40 (s, 3H, CH_3), 2.93-3.01 (m, 3H, H-piperidine), 3.53 (s, 2H, CH_2-benzyl), 7.26-7.28 (m, 2H, H_3, H_5-phenyl), 7.32-7.33 (m, 5H, H_2, H_3, H_4, H_5, H_6-benzyl), 7.95-7.97 (m, 2H, H_2, H_6-phenyl); ^{13}C NMR ($CDCl_3$, 100 MHz) δ: 21.55 (CH_3), 29.54 ($2CH_2$), 34.62 (CH), 52.74 ($2CH_2$), 63.18 (CH_2), 124.13 (C), 127.04 (2CH), 127.31 (CH), 128.23 (2CH), 129.02 (2CH), 129.49 (2CH), 138.28 (C), 141.31 (C), 168.15 (C), 181.86 (C); Anal. calcd for $C_{21}H_{23}N_3O$: C, 75.65; H, 6.95; N, 12.60, found: C, 75.87; H, 6.92; N, 12.56.

4.1.3.3 5-(1-benzylpiperidin-4-yl)-3-(4-chlorophenyl)-1,2,4-oxadiazole (6c)

Light yellow powder; yield: 32.1 %; mp: 106-108 °C; IR (KBr, cm^{-1}): 1592 (C=N), 1139 (C-O); LC-MS $[M + 1]^+$: m/z 354; ^1H NMR ($CDCl_3$, 400 MHz) δ: 2.00-2.19 (m, 6H, H-piperidine), 2.94-3.02 (m, 3H, H-piperidine), 3.54 (s, 2H, CH_2-benzyl), 7.26-7.34 (m, 5H, H_2, H_3, H_4, H_5, H_6-benzyl), 7.44-7.46 (m, 2H, H_3, H_5-phenyl), 8.00-8.02 (m, 2H, H_2, H_6-phenyl); ^{13}C NMR ($CDCl_3$, 100 MHz) δ: 29.53 ($2CH_2$), 34.61 (CH), 52.71 ($2CH_2$), 63.18 (CH_2), 125.47 (C), 127.08 (2CH), 128.75 (CH), 128.72 (2CH), 129.04 (2CH), 129.12 (2CH), 137.17 (C), 138.23 (C), 167.39 (C), 182.30 (C); Anal. calcd for $C_{20}H_{20}ClN_3O$: C, 67.89; H, 5.70; N, 11.88, found: C, 68.12; H, 5.69; N, 11.82.

4.1.3.4 5-(1-benzylpiperidin-4-yl)-3-(4-fluorophenyl)-1,2,4-oxadiazole (6d)

Light yellow powder; yield: 40.7 %; mp: 92.7-93.6 °C; IR (KBr, cm^{-1}): 1571 (C=N), 1130 (C-O); LC-MS $[M + 1]^+$: m/z 337.9; ^1H NMR ($CDCl_3$, 400 MHz) δ: 1.93-2.12 (m, 6H, H-piperidine), 2.87-2.93 (m, 3H, H-piperidine), 3.47 (s, 2H, CH_2-benzyl), 7.06-7.10 (m, 2H, H_3, H_5-phenyl), 7.18-7.26 (m, 5H, H_2, H_3, H_4, H_5, H_6-benzyl), 7.98-8.01 (m, 2H, H_2, H_6-phenyl); ^{13}C NMR ($CDCl_3$, 100 MHz) δ: 29.55 ($2CH_2$), 34.61 (CH), 52.73 ($2CH_2$), 63.20 (CH_2), 115.90 (C), 123.23 (2CH), 127.12 (CH), 128.28 (2CH), 129.08 (2CH), 129.54 (2CH), 129.62 (C), 138.24 (C), 165.67 (C), 182.21 (C); Anal. calcd for $C_{20}H_{20}FN_3O$: C, 71.20; H, 5.97; N, 12.45, found: C, 71.41; H, 5.99; N, 12.40.

4.1.3.5 5-(1-(4-fluorobenzyl)piperidin-4-yl)-3-phenyl-1,2,4-oxadiazole (6e)

Light yellow powder; yield: 20.9 %; mp: 93.4-94.5 °C; IR (KBr, cm^{-1}): 1596 (C=N), 1214 (C-O); LC-MS $[M + 1]^+$: m/z 338; ^1H NMR ($CDCl_3$, 400 MHz) δ: 1.97-2.07 (m, 4H, H-piperidine), 2.11-2.19 (m, 4H, H-piperidine), 2.92-3.05 (m, 1H, H-piperidine), 3.50 (s, 2H, CH_2-benzyl), 7.01 (t, 2H, J = 8 Hz, H_3, H_5-benzyl), 7.26-7.32 (m, 2H, H_2, H_6-benzyl), 7.45-7.50 (m, 3H, H_3, H_4, H_5-phenyl), 8.08 (d, 2H, J = 8 Hz, H_2, H_6-phenyl); ^{13}C NMR ($CDCl_3$, 100 MHz) δ: 29.53 ($2CH_2$), 34.60 (CH), 52.65 ($2CH_2$), 62.35 (CH_2), 115.15 (2CH), 126.95 (C), 127.42 (2CH), 128.81 (2CH), 130.40 (2CH), 131.08 (CH), 133.98 (C), 160.79 (C), 168.20 (C), 182.00 (C); Anal. calcd for $C_{20}H_{20}FN_3O$: C, 71.20; H, 5.97; N, 12.45, found: C, 71.40; H, 5.94; N, 12.48.

4.1.3.6 5-(1-(4-fluorobenzyl)piperidin-4-yl)-3-(p-tolyl)-1,2,4-oxadiazole (6f)

White powder; yield: 56.3 %; mp: 90-90.8 °C; IR (KBr, cm^{-1}): 1582 (C=N), 1223 (C-O), 1344,1440 (CH_3); LC-MS $[M + 1]^+$: m/z 351.9; ^1H NMR ($CDCl_3$, 400 MHz) δ: 2.02-2.17 (m, 6H, H-piperidine), 2.40 (s, 3H, CH_3), 2.90-3.01 (m, 3H, H-piperidine), 3.49 (s, 2H, CH_2-benzyl), 6.98-7.03 (m, 2H, H_3, H_5-benzyl), 7.26-7.31 (m, 4H, H_2, H_6-benzyl, H_3, H_5-phenyl), 7.95 (d, 2H, *J* = 8 Hz, H_2, H_6-phenyl); ^{13}C NMR ($CDCl_3$, 100 MHz) δ: 21.55 (CH_3), 29.53 ($2CH_2$), 34.59 (CH), 52.65 ($2CH_2$), 62.34 (CH_2), 115.13 (2CH), 124.13 (C), 127.33 (2CH), 129.51 (2CH), 130.46 (2CH), 134.04 (CH), 141.35 (C), 160.77 (C), 168.18 (C), 181.81 (C); Anal. calcd for $C_{21}H_{22}FN_3O$: C, 71.77; H, 6.31; N, 11.96, found: C, 72.01; H, 6.32; N, 11.91.

4.1.3.7 3-(4-chlorophenyl)-5-(1-(4-fluorobenzyl)piperidin-4-yl)-1,2,4-oxadiazole (6g)

Light yellow powder; yield: 36.0 %; mp: 106.7-107.7 °C; IR (KBr, cm^{-1}): 1596 (C=N), 1153 (C-O); LC-MS $[M + 1]^+$: m/z 372; ^1H NMR ($CDCl_3$, 400 MHz) δ: 1.96-2.06 (m, 4H, H-piperidine), 2.10-2.19 (m, 4H, H-piperidine), 2.91-3.02 (m, 1H, H-piperidine), 3.50 (s, 2H, CH_2-benzyl), 7.01 (t, 2H, *J* = 8 Hz, H_3, H_5-benzyl), 7.26-7.31 (m, 2H, H_2, H_6-benzyl), 7.44 (d, 2H, *J* = 8 Hz, H_3, H_5-phenyl), 8.02 (d, 2H, *J* = 8 Hz, H_2, H_6-phenyl); ^{13}C NMR ($CDCl_3$, 100 MHz) δ: 29.52 ($2CH_2$), 34.59 (CH), 52.62 ($2CH_2$), 62.34 (CH_2), 115.16 (2CH), 125.48 (C), 128.73 (2CH), 130.39 (2CH), 133.96 (2CH), 137.21 (C), 160.80 (C), 163.23 (C), 167.42 (C), 182.24 (C); Anal. calcd for $C_{20}H_{19}ClFN_3O$: C, 64.60; H, 5.15; N, 11.30, found: C, 64.84; H, 5.14; N, 11.23.

4.1.3.8 5-(1-(4-fluorobenzyl)piperidin-4-yl)-3-(4-fluorophenyl)-1,2,4-oxadiazole (6h)

Light yellow powder; yield: 31.6 %; mp: 115.7-117.7 °C; IR (KBr, cm^{-1}): 1609 (C=N), 1230 (C-O); LC-MS $[M + 1]^+$: m/z 355.8; ^1H NMR ($CDCl_3$, 400 MHz) δ: 1.90-2.11 (m, 6H, H-piperidine), 2.84-2.95 (m, 3H, H-piperidine), 3.43 (s, 2H, CH_2-benzyl), 6.91-6.96 (m, 2H, H_3, H_5-benzyl), 7.08 (t, 2H, *J* = 8 Hz, H_3, H_5-phenyl), 7.19-7.24 (m, 2H, H_2, H_6-benzyl), 7.98-8.02 (m, 2H, H_2, H_6-phenyl); ^{13}C NMR ($CDCl_3$, 100 MHz) δ: 29.52 ($2CH_2$), 34.57 (CH), 52.63 ($2CH_2$), 62.35 (CH_2), 115.90 (2CH), 123.20 (2CH), 129.53 (C), 130.43 (2CH), 133.97 (2CH), 160.81 (C), 163.27 (C), 165.77 (C), 167.41 (C), 182.13 (C); Anal. calcd for $C_{20}H_{19}F_2N_3O$: C, 67.59; H, 5.39; N, 11.82, found: C, 67.82; H, 5.36; N, 11.76.

4.1.3.9 5-(1-(4-chlorobenzyl)piperidin-4-yl)-3-phenyl-1,2,4-oxadiazole (6i)

Light yellow powder; yield: 39.4 %; mp: 95.6-96.7 °C; IR (KBr, cm^{-1}): 1586 (C=N), 1110 (C-O); LC-MS $[M + 1]^+$: m/z 353.8; ^1H NMR ($CDCl_3$, 400 MHz) δ: 1.96-2.18 (m, 6H, H-piperidine), 2.89-3.02 (m, 3H, H-piperidine), 3.48 (s, 2H, CH_2-benzyl), 7.25-7.30 (m, 4H, H_2, H_3, H_5, H_6-benzyl), 7.46-7.48 (m, 3H, H_3, H_4, H_5-phenyl), 8.06-8.08 (m, 2H, H_2, H_6-phenyl); ^{13}C NMR ($CDCl_3$, 100 MHz) δ: 29.50 ($2CH_2$), 34.51 (CH), 52.65 ($2CH_2$), 62.33 (CH_2), 126.93 (C), 127.33 (2CH), 127.42 (2CH), 128.37 (2CH), 130.22 (2CH), 131.05 (CH), 132.70 (C), 136.89 (C), 168.16 (C), 181.94 (C); Anal. calcd for $C_{20}H_{20}ClN_3O$: C, 67.89; H, 5.70; N, 11.88, found: C, 68.12; H, 5.68; N, 11.93.

4.1.3.10 5-(1-(4-chlorobenzyl)piperidin-4-yl)-3-(p-tolyl)-1,2,4-oxadiazole (6j)

Light yellow powder; yield: 40.3 %; mp: 103.5-104.7 °C; IR (KBr, cm^{-1}): 1582 (C=N), 1213 (C-O), 1358,1486 (CH_3); LC-MS $[M + 1]^+$: m/z 367.8; ^1H NMR ($CDCl_3$, 400 MHz) δ: 1.89-2.11 (m, 6H, H-piperidine), 2.33 (s, 3H, CH_3), 2.82-2.94 (m, 3H, H-piperidine), 3.42 (s, 2H, CH_2-benzyl), 7.18-7.23 (m, 6H, H_2, H_3, H_5, H_6-benzyl, H_3, H_5-phenyl), 7.87 (d, 2H, *J* = 8 Hz, H_2, H_6-phenyl); ^{13}C NMR ($CDCl_3$, 100 MHz) δ: 21.59 (CH_3), 29.52 ($2CH_2$), 34.55 (CH), 52.70 ($2CH_2$), 62.37 (CH_2), 124.13 (C), 127.35 (2CH), 128.43 (2CH), 129.54 (2CH), 130.28 (2CH), 132.78 (C), 136.89 (C), 141.39 (C), 168.22 (C), 181.78 (C); Anal. calcd for $C_{21}H_{22}ClN_3O$: C, 68.56; H, 6.03; N, 11.42, found: C, 68.79; H, 6.01; N, 11.37.

4.1.3.11 5-(1-(4-chlorobenzyl)piperidin-4-yl)-3-(4-chlorophenyl)-1,2,4-oxadiazole (6k)

Light yellow powder; yield: 51.7 %; mp: 110.7-113.7 °C; IR (KBr, cm^{-1}): 1582 (C=N), 1213 (C-O); LC-MS $[M + 1]^+$: m/z 387.8; ^1H NMR ($CDCl_3$, 400 MHz) δ: 1.88-2.11 (m, 6H, H-piperidine), 2.82-2.95 (m, 3H, H-piperidine), 3.41 (s, 2H, CH_2-benzyl), 7.18-7.22 (m, 4H, H_2, H_3, H_5, H_6-benzyl), 7.35 (d, 2H, J = 8 Hz, H_3, H_5-phenyl), 7.92 (d, 2H, J = 8 Hz, H_2, H_6-phenyl); ^{13}C NMR ($CDCl_3$, 100 MHz) δ: 29.47 ($2CH_2$), 34.50 (CH), 52.63 ($2CH_2$), 62.36 (CH_2), 125.45 (C), 128.75 (2CH), 129.16 (2CH), 129.46 (2CH), 130.32 (2CH), 132.82 (C), 136.73 (C), 137.23 (C), 167.41 (C), 182.19 (C); Anal. calcd for $C_{20}H_{19}Cl_2N_3O$: C, 61.86; H, 4.93; N, 10.82, found: C, 62.09; H, 4.91; N, 10.78.

4.1.3.12 5-(1-(4-chlorobenzyl)piperidin-4-yl)-3-(4-fluorophenyl)-1,2,4-oxadiazole (6l)

Light yellow powder; yield: 40.7 %; mp: 89.9-90.4 °C; IR (KBr, cm^{-1}): 1600 (C=N), 1221 (C-O); LC-MS $[M + 1]^+$: m/z 371.8; ^1H NMR ($CDCl_3$, 400 MHz) δ: 1.99-2.19 (m, 6H, H-piperidine), 2.90-3.02 (m, 3H, H-piperidine), 3.49 (s, 2H, CH_2-benzyl), 7.13-7.18 (m, 2H, H_3, H_5-phenyl), 7.26-7.29 (m, 4H, H_2, H_3, H_5, H_6-benzyl), 8.05-8.09 (m, 2H, H_2, H_6-phenyl); ^{13}C NMR ($CDCl_3$, 100 MHz) δ: 29.51 ($2CH_2$), 34.51 (CH), 52.66 ($2CH_2$), 62.35 (CH_2), 115.88 (2CH), 123.16 (C), 129.51 (2CH), 130.23 (2CH), 132.74 (2CH), 136.86 (C), 163.24 (C), 165.73 (C), 167.37 (C), 182.09 (C); Anal. calcd for $C_{20}H_{19}ClFN_3O$: C, 64.60; H, 5.15; N, 11.30, found: C, 64.81; H, 5.12; N, 11.37.

4.1.3.13 5-(1-(2-chlorobenzyl)piperidin-4-yl)-3-phenyl-1,2,4-oxadiazole (6m)

Light yellow powder; yield: 28.6 %; mp: 61.5-62.2 °C; IR (KBr, cm^{-1}): 1583 (C=N), 1134 (C-O); LC-MS $[M + 1]^+$: m/z 354; ^1H NMR ($CDCl_3$, 400 MHz) δ: 2.01-2.18 (m, 6H, H-piperidine), 2.93-3.02 (m, 3H, H-piperidine), 3.50 (s, 2H, CH_2-benzyl), 7.13-7.15 (m, 3H, H_4, H_5, H_6-benzyl), 7.21-7.25 (m, 3H, H_3, H_4, H_5-phenyl), 7.44-7.49 (m, 1H, H_3-benzyl), 8.06 (d, 2H, J = 8 Hz, H_2, H_6-phenyl); ^{13}C NMR ($CDCl_3$, 100 MHz) δ: 29.56 ($2CH_2$), 34.67 (CH), 52.69 ($2CH_2$), 62.92 (CH_2), 126.89 (C), 127.00 (CH), 127.42 (2CH), 128.79 (2CH), 128.93 (2CH), 129.04 (CH), 131.04 (CH), 135.14 (C), 136.66 (C), 168.18 (C), 182.09 (C); Anal. calcd for $C_{20}H_{20}ClN_3O$: C, 67.89; H, 5.70; N, 11.88, found: C, 68.13; H, 5.67; N, 11.80.

4.1.3.14 5-(1-(2-chlorobenzyl)piperidin-4-yl)-3-(p-tolyl)-1,2,4-oxadiazole (6n)

White powder; yield: 33.8 %; mp: 121.8-124.7 °C; IR (KBr, cm^{-1}): 1582 (C=N), 1146 (C-O), 1442,1350 (CH_3); LC-MS $[M + 1]^+$: m/z 367.9; ^1H NMR ($CDCl_3$, 400 MHz) δ: 2.09-2.14 (m, 4H, H-piperidine), 2.24-2.31 (m, 2H, H-piperidine), 2.40 (s, 3H, CH_3), 2.97-3.04 (m, 3H, H-piperidine), 3.65 (s, 2H, CH_2-benzyl), 7.17-7.28 (m, 3H, H_4, H_5, H_6-benzyl), 7.34 (d, 2H, J = 8 Hz, H_3, H_5-phenyl), 7.50-7.51 (m, 1H, H_3-benzyl), 7.95 (d, 2H, J = 8 Hz, H_2, H_6-phenyl); ^{13}C NMR ($CDCl_3$, 100 MHz) δ: 21.56 (CH_3), 29.62 ($2CH_2$), 34.56 (CH), 52.85 ($2CH_2$), 59.34 (CH_2), 124.14 (C), 126.62 (2CH), 127.33 (CH), 128.07 (2CH), 129.51 (2CH), 130.48 (CH), 134.19 (C), 136.05 (C), 141.33 (C), 168.18 (C), 181.85 (C); Anal. calcd for $C_{21}H_{22}ClN_3O$: C, 68.56; H, 6.03; N, 11.42, found: C, 68.75; H, 5.99; N, 11.38.

4.1.3.15 5-(1-(2-chlorobenzyl)piperidin-4-yl)-3-(4-chlorophenyl)-1,2,4-oxadiazole (6o)

White powder; yield: 33.8 %; mp: 85.5-87 °C; IR (KBr, cm^{-1}): 1597 (C=N), 1141 (C-O); LC-MS $[M + 1]^+$: m/z 387.8; ^1H NMR ($CDCl_3$, 400 MHz) δ: 1.95-2.07 (m, 4H, H-piperidine), 2.19-2.24 (m, 2H, H-piperidine), 2.90-2.97 (m, 3H, H-piperidine), 3.58 (s, 2H, CH_2-benzyl), 7.14-7.19 (m, 2H, H_4, H_5-benzyl), 7.27 (d, 1H, J = 8 Hz ,H_3-benzyl), 7.36 (d, 2H, J = 8 Hz, H_3, H_5-phenyl), 7.42 (d, 1H, J = 8 Hz ,H_6-benzyl), 7.93 (d, 2H, J = 8 Hz, H_2, H_6-phenyl); ^{13}C NMR ($CDCl_3$, 100 MHz) δ: 29.60 ($2CH_2$), 34.55 (CH), 52.81 ($2CH_2$), 59.35 (CH_2), 125.50 (C), 126.67 (CH), 128.16 (2CH), 129.16 (2CH), 129.45 (2CH), 130.54 (CH), 134.25 (C), 135.99 (C), 137.21 (C), 167.43 (C), 182.28 (C); Anal. calcd for $C_{20}H_{19}Cl_2N_3O$: C, 61.86; H, 4.93; N, 10.82, found: C, 62.09; H, 4.92; N, 10.75.

EXCLI Journal 2021;20:907-921 – ISSN 1611-2156
Received: February 27, 2021, accepted: May 10, 2021, published: May 18, 2021

4.1.3.16 5-(1-(2-chlorobenzyl)piperidin-4-yl)-3-(4-fluorophenyl)-1,2,4-oxadiazole (6p)

Light yellow powder; yield: 30.5 %; mp: 69.5-70 °C; IR (KBr, cm^{-1}): 1600 (C=N), 1212 (C-O); LC-MS $[M + 1]^+$: m/z 371.8; ^1H NMR ($CDCl_3$, 400 MHz) δ: 2.05-2.17 (m, 4H, H-piperidine), 2.29-2.34 (m, 2H, H-piperidine), 3.00-3.03 (m, 3H, H-piperidine), 3.68 (s, 2H, CH_2-benzyl), 7.20-7.29 (m, 3H, H_4, H_5, H_6-benzyl), 7.37 (d, 2H, *J* = 8 Hz, H_3, H_5-phenyl), 7.53-7.54 (m, 1H, H_3-benzyl), 8.08-8.12 (m, 2H, H_2, H_6-phenyl); ^{13}C NMR ($CDCl_3$, 100 MHz) δ: 29.61 ($2CH_2$), 34.54 (CH), 52.82 ($2CH_2$), 59.35 (CH_2), 115.90 (C), 123.22 (CH), 126.66 (2CH), 128.15 (2CH), 129.45 (2CH), 130.54 (CH), 134.24 (C), 136.00 (C), 163.27 (C), 167.41 (C), 182.18 (C); Anal. calcd for $C_{20}H_{19}ClFN_3O$: C, 64.60; H, 5.15; N, 11.30, found: C, 64.79; H, 5.13; N, 11.23.

4.1.3.17 5-(1-(4-methylbenzyl)piperidin-4-yl)-3-phenyl-1,2,4-oxadiazole (6q)

Light yellow powder; yield: 32.8 %; mp: 90.3-91.4 °C; IR (KBr, cm^{-1}): 1589 (C=N), 1145 (C-O), 1363,1440 (CH_3); LC-MS $[M + 1]^+$: m/z 334; ^1H NMR ($CDCl_3$, 400 MHz) δ: 2.09-2.14 (m, 6H, H-piperidine), 2.26-2.31 (m, 3H, CH_3), 2.98-3.05 (m, 3H, H-piperidine), 3.65 (s, 2H, CH_2-benzyl), 7.17-7.27 (m, 2H, H_3, H_5-benzyl), 7.34 (d, 2H, *J* = 8 Hz, H_2, H_6-benzyl),7.47-7.52 (m, 3H, H_3, H_4, H_5-phenyl), 8.07 (d, 2H, *J* = 8 Hz, H_2, H_6-phenyl); ^{13}C NMR ($CDCl_3$, 100 MHz) δ: 21.55 (CH_3), 29.62 ($2CH_2$), 34.56 (CH), 52.84 ($2CH_2$), 59.35 (CH_2), 126.63 (C), 127.42 (2CH), 128.80 (2CH), 129.41 (2CH), 130.50 (2CH), 131.06 (CH), 134.21 (C), 136.04 (C), 168.20 (C), 182.04 (C); Anal. calcd for $C_{21}H_{23}N_3O$: C, 75.65; H, 6.95; N, 12.60, found: C, 75.86; H, 6.94; N, 12.55.

4.1.3.18 5-(1-(4-methylbenzyl)piperidin-4-yl)-3-(p-tolyl)-1,2,4-oxadiazole (6r)

Light yellow powder; yield: 47.2 %; mp: 84.5-85.3 °C; IR (KBr, cm^{-1}): 1579 (C=N), 1117 (C-O), 1358,1410 (CH_3); LC-MS $[M + 1]^+$: m/z 347.9; ^1H NMR ($CDCl_3$, 400 MHz) δ: 2.02-2.15 (m, 6H, H-piperidine), 2.33 (s , 3H , CH_3-benzyl), 2.39 (s , 3H , CH_3-phenyl), 2.92-2.96 (m, 3H, H-piperidine), 3.49 (s, 2H, CH_2-benzyl), 7.12 (d, 2H, *J* = 8 Hz, H_3, H_5-benzyl), 7.20 (d, 2H, *J* = 8 Hz, H_2, H_6-benzyl), 7.25 (d, 2H, *J* = 8 Hz, H_3, H_5-phenyl), 7.95 (d, 2H, *J* = 8 Hz, H_2, H_6-phenyl); ^{13}C NMR ($CDCl_3$, 100 MHz) δ: 21.10 (CH_3), 21.54 (CH_3), 29.54 ($2CH_2$), 34.64 (CH), 52.68 ($2CH_2$), 62.90 (CH_2), 124.15 (C), 127.31 (2CH), 128.91 (2CH), 129.00 (2CH), 129.48 (2CH), 135.15 (C), 136.60 (C), 141.28 (C), 168.14 (C), 181.88 (C); Anal. calcd for $C_{22}H_{25}N_3O$: C, 76.05; H, 7.25; N, 12.09, found: C, 76.28; H, 7.23; N, 12.02.

4.1.3.19 3-(4-chlorophenyl)-5-(1-(4-methylbenzyl)piperidin-4-yl)-1,2,4-oxadiazole (6s)

Light yellow powder; yield: 47.3 %; mp: 111.4-112.5 °C; IR (KBr, cm^{-1}): 1585 (C=N), 1128 (C-O), 1361,1446 (CH_3); LC-MS $[M + 1]^+$: m/z 367.8; ^1H NMR ($CDCl_3$, 400 MHz) δ: 1.95-2.10 (m, 6H, H-piperidine), 2.26 (s, 3H, CH_3), 2.86-2.91 (m, 3H, H-piperidine), 3.43 (s, 2H, CH_2-benzyl), 7.05 (d, 2H, *J* = 8 Hz, H_3, H_5-benzyl), 7.15 (d, 2H, *J* = 8 Hz, H_2, H_6-benzyl), 7.35 (d, 2H, *J* = 8 Hz, H_3, H_5-phenyl), 7.92 (d, 2H, *J* = 8 Hz, H_2, H_6-phenyl); ^{13}C NMR ($CDCl_3$, 100 MHz) δ: 21.15 (CH_3), 29.55 ($2CH_2$), 34.66 (CH), 52.68 ($2CH_2$), 62.93 (CH_2), 125.53 (C), 128.76 (2CH), 128.97 (2CH), 129.07 (2CH), 129.15 (2CH), 135.09 (C), 136.72 (C), 137.19 (C), 167.42 (C), 182.35 (C); Anal. calcd for $C_{21}H_{22}ClN_3O$: C, 68.56; H, 6.03; N, 11.42, found: C, 68.79; H, 6.01; N, 11.38.

4.1.3.20 3-(4-fluorophenyl)-5-(1-(4-methylbenzyl)piperidin-4-yl)-1,2,4-oxadiazole (6t)

Light yellow powder; yield: 48.2 %; mp: 96.5-97.2 °C; IR (KBr, cm^{-1}): 1600 (C=N), 1223 (C-O), 1352,1444 (CH_3); LC-MS $[M + 1]^+$: m/z 351.7; ^1H NMR ($CDCl_3$, 400 MHz) δ: 1.99-2.17 (m, 6H, H-piperidine), 2.34 (s, 3H, CH_3), 2.94-2.98 (m, 3H, H-piperidine), 3.50 (s, 2H, CH_2-benzyl), 7.13-7.17 (m, 4H, H_2, H_3, H_5, H_6-benzyl), 7.23 (t, 2H, *J* = 8 Hz, H_3, H_5-phenyl), 8.05-8.09 (m, 2H, H_2, H_6-phenyl); ^{13}C NMR ($CDCl_3$, 100 MHz) δ: 21.11 (CH_3), 29.54 ($2CH_2$), 34.64 (CH),

52.67 ($2CH_2$), 62.92 (CH_2), 115.86 (2CH), 123.20 (C), 128.93 (2CH), 129.51 (2CH), 135.09 (2CH), 136.68 (C), 163.23 (C), 165.72 (C), 167.36 (C), 182.22 (C); Anal. calcd for $C_{21}H_{22}FN_3O$: C, 71.77; H, 6.31; N, 11.96, found: C, 72.02; H, 6.30; N, 11.87.

4.2 Inhibitory activity against AChE and BuChE enzymes

Acetylcholinesterase inhibitory activity was determined using the 5,5-dithiobis-2-nitrobenzoic acid (DTNB) assay as described by Ellman et al. (1961). AChE (E.C. 3.1.1.7, type V-S, lyophilized powder, from the electric eel, 1000 units) and BuChE (E.C. 3.1.1.8, from equine serum), acetylthiocholine iodide (ATCI), butyrylthiocholine iodide (BTCI), and 5,5-dithiobis-(2-nitrobenzoic acid) (DTNB) were all acquired from Sigma-Aldrich. Potassium dihydrogen phosphate, dipotassium hydrogen phosphate, potassium hydroxide, and sodium hydrogen carbonate were obtained from Fluka. Donepezil was used as a reference compound. Assay solutions were then prepared by the addition of compounds **6a-t** to a mixture containing DMSO (5 mL) and methanol (5mL) diluted in potassium phosphate buffer (0.1 M, pH=8.0). In this regard, each one of the wells included a 50 µL potassium phosphate buffer, 25 µL sample dissolved in 50 % methanol and 50 % DMSO, and 25 µL enzyme (the final concentration 0.22 U/mL in buffer). Thereafter, the wells were pre-incubated for 15 min at room temperature, and 125 µL DTNB (3 mM in buffer) was added to each plate. Followed by the addition of substrate (ATCI 3 mM in water), the absorbance change was measured using a 96-well plate reader (BioTek ELx808) at 405 nm after 15 min. As well, the IC_{50} values were expressed as mean ± SD. The percentage of enzyme's inhibition was calculated by comparing with a blank sample (100 % activity). The described method was also used for the BuChE inhibition assay.

4.3 Docking study

The AutoDock Tools version 1.5.6rc3 (http://mgltools.scripps.edu) was applied for docking study of the compound **6n**. In the current study, the X-ray crystallographic structure of BuChE (PDB code 1P0I) was obtained from the Protein Data Bank. Subsequently, all water molecules in the PDB file were removed, hydrogen atoms were added to amino acid residues, and Gasteiger charges were assigned to all atoms of the enzyme. The structure of the compound **6n** was optimized by the MM+ force field using HyperChem8 (http://www.hyper.com) and then converted to pdbqt format file using AutoDock Tools. The grid size was set at $40 \times 40 \times 40$ with a grid spacing of 0.375 Å, and the grid center was determined at dimensions (x, y, and z): 137.44, 114.33, and 39.22, respectively. Each docked system was performed by 100 runs of the AutoDock search using the Lamarckian genetic algorithm (LGA). Finally, the lowest energy conformations were selected for analyzing the interactions between the enzyme and inhibitor. Moreover, graphic manipulations and visualizations were done by Pymol software version 1.5.0.1 (http://pymol.findmysoft.com).

4.4 ADME properties

The ADME properties of the synthesized compounds in this study were predicted using the SwissADME online property calculator (http://www.swissadme.ch.) (Daina et al., 2017). Notably, topological polar surface area (TPSA), number of rotatable bonds (*n*-ROTB), molecular weight (MW), the logarithm of the partition coefficient (miLog *P*), number of hydrogen bond acceptors (*n*-ON), number of hydrogen bond donors (*n*-OHNH), and Lipinski's rule of five criteria were calculated as well (Lipinski et al., 2001). Additionally, the following equation was utilized to calculate the intestinal absorption percent (% ABS): $\% ABS = 109 - (0.345 \times TPSA)$ (Zhao et al., 2002).

Acknowledgments

This work was supported by a grant from the Research Council of Shahid Beheshti University of Medical Sciences (Grant No; 7763).

REFERENCES

Alzheimer's Association. 2013 Alzheimer's disease facts and figures. Alzheimer's and Dementia. 2013;9:208–45. doi: 10.1016/j.jalz.2013.02.003.

Alzheimer's Association. 2017 Alzheimer's disease facts and figures. Alzheimer's and Dementia. 2017;13:325–73.

Alzheimer's Disease International. World Alzheimer Report 2019: Attitudes to dementia. London: Alzheimer's Disease International, 2019. https://www.alzint.org/u/WorldAlzheimerReport2019.pdf.

Amenta F, Tayebati S. Pathways of acetylcholine synthesis, transport and release as targets for treatment of adult-onset cognitive dysfunction. Curr Med Chem. 2008;15:488–98. doi: 10.2174/092986708783503203.

Anand R, Gill KD, Mahdi AA. Therapeutics of Alzheimer's disease: Past, present and future. Vol. 76, Neuropharmacology. 2014;76:27–50. doi: 10.1016/j.neuropharm.2013.07.004.

Busche MA, Hyman BT. Synergy between amyloid-β and tau in Alzheimer's disease. Nat Neurosci. 2020;23:1183–93. doi: 10.1038/s41593-020-0687-6.

Cass SP. Alzheimer's disease and exercise: A literature review. Curr Sports Med Rep. 2017;16:19–22. doi: 10.1249/JSR.0000000000000332.

Coman H, Nemeş B. New therapeutic targets in Alzheimer's disease. Int J Gerontol. 2017;11:2–6. doi: 10.1016/j.ijge.2016.07.003.

Daina A, Michielin O, Zoete V. SwissADME: A free web tool to evaluate pharmacokinetics, drug-likeness and medicinal chemistry friendliness of small molecules. Sci Rep. 2017;7:42717. doi: 10.1038/srep42717.

Darvesh S, Hopkins DA, Geula C. Neurobiology of butyrylcholinesterase. Nat Rev Neurosci. 2003;4:131–8. doi: 10.1038/nrn1035.

de Andrade P, Mantoani SP, Gonçalves Nunes PS, Magadán CR, Pérez C, Xavier DJ, et al. Highly potent and selective aryl-1,2,3-triazolyl benzylpiperidine inhibitors toward butyrylcholinesterase in Alzheimer's disease. Bioorg Med Chem. 2019;27:931–43. doi: 10.1016/j.bmc.2018.12.030.

Ellman GL, Courtney KD, Andres V, Featherstone RM. A new and rapid colorimetric determination of acetylcholinesterase activity. Biochem Pharmacol. 1961;7:88-95. doi: 10.1016/0006-2952(61)90145-9.

Ertl P, Rohde B, Selzer P. Fast calculation of molecular polar surface area as a sum of fragment-based contributions and its application to the prediction of drug transport properties. J Med Chem. 2000;43:3714–7. doi: 10.1021/jm000942e.

Femminella GD, Thayanandan T, Calsolaro V, Komici K, Rengo G, Corbi G, et al. Imaging and molecular mechanisms of Alzheimer's disease: A review. Int J Mol Sci. 2018;19:3702. doi: 10.3390/ijms19123702.

Franjesevic AJ, Sillart SB, Beck JM, Vyas S, Callam CS, Hadad CM. Resurrection and reactivation of acetylcholinesterase and butyrylcholinesterase. Chemistry. 2019;25:5337–71. doi: 10.1002/chem.201805075.

Hampel H, Mesulam MM, Cuello AC, Farlow MR, Giacobini E, Grossberg GT, et al. The cholinergic system in the pathophysiology and treatment of Alzheimer's disease. Brain. 2018;141:1917–33. doi: 10.1093/brain/awy132.

Hampel H, Mesulam MM, Cuello AC, Khachaturian AS, Vergallo A, Farlow MR, et al. Revisiting the cholinergic hypothesis in Alzheimer's disease: Emerging evidence from translational and clinical research. J Prev Alzheimer's Dis. 2019;6(1):2-15. doi: 10.14283/jpad.2018.43.

Joubert J, Kapp E. Discovery of 9-phenylacridinediones as highly selective butyrylcho-linesterase inhibitors through structure-based virtual screening. Bioorg Med Chem Lett. 2020;30:127075. doi: 10.1016/j.bmcl.2020.127075.

Li Q, Yang H, Chen Y, Sun H. Recent progress in the identification of selective butyrylcholinesterase inhibitors for Alzheimer's disease. Eur J Med Chem. 2017; 132:294-309. Doi: 10.1016/j.ejmech.2017.03.062.

Lipinski CA, Lombardo F, Dominy BW, Feeney PJ. Experimental and computational approaches to estimate solubility and permeability in drug discovery and development settings. Adv Drug Deliv Rev. 2001;46:3–26. doi: 10.1016/s0169-409x(00)00129-0.

Oboudiyat C, Glazer H, Seifan A, Greer C, Isaacson RS. Alzheimer's disease. Semin Neurol. 2013;33:313–29. doi: 10.1055/s-0033-1359319.

Richter N, Beckers N, Onur OA, Dietlein M, Tittgemeyer M, Kracht L, et al. Effect of cholinergic treatment depends on cholinergic integrity in early Alzheimer's disease. Brain. 2018;141:903–15. doi: 10.1093/brain/awx356.

Sawatzky E, Wehle S, Kling B, Wendrich J, Bringmann G, Sotriffer CA, et al. Discovery of highly selective and nanomolar carbamate-based butyrylcholinesterase inhibitors by rational investigation into their inhibition mode. J Med Chem. 2016;59:2067–82. doi: 10.1021/acs.jmedchem.5b01674.

Sengoku R. Aging and Alzheimer's disease pathology. Neuropathology. 2020;40:22-9. doi: 10.1111/neup.12626.

Sharma K. Cholinesterase inhibitors as Alzheimer's therapeutics (Review). Mol Med Rep. 2019;20:1479-87. doi: 10.3892/mmr.2019.10374.

Soria Lopez JA, González HM, Léger GC. Alzheimer's disease. In: Handb Clin Neurol. 2019;167: 231-255. doi: 10.1016/B978-0-12-804766-8.00013-3.

Sugimoto H, Yamanish Y, Iimura Y, Kawakami Y. Donepezil hydrochloride (E2020) and other acetylcholinesterase inhibitors. Curr Med Chem. 2012;7:303–39. doi: 10.2174/0929867003375191.

van Greunen DG, Cordier W, Nell M, van der Westhuyzen C, Steenkamp V, Panayides J-L, et al. Targeting Alzheimer's disease by investigating previ-ously unexplored chemical space surrounding the cholinesterase inhibitor donepezil. Eur J Med Chem. 2017;127:671–90. doi: 10.1016/j.ejmech.2016.10.036.

Vaz M, Silvestre S. Alzheimer's disease: Recent treatment strategies. Eur J Pharmacol. 2020;887:173554. doi: 10.1016/j.ejphar.2020.173554.

Wajid S, Khatoon A, Khan MA, Zafar H, Kanwal S, Atta-ur-Rahman, et al. Microwave-assisted organic synthesis, structure–activity relationship, kinetics and molecular docking studies of non-cytotoxic benzamide derivatives as selective butyrylcholinesterase inhibitors. Bioorg Med Chem. 2019;27:4030–40. doi: 10.1016/j.bmc.2019.07.015.

Wu C, Tu Y-b, Li Z, Li Y-f. Highly selective carbamate-based butyrylcholinesterase inhibitors derived from a naturally occurring pyranoisoflavone. Bioorg Chem. 2019;88:102949. doi: 10.1016/j.bioorg.2019.102949.

Zavareh E, Hedayati M, Rad L, Kiani A, Shahhosseini S, Faizi M, et al. Design, synthesis and biological evaluation of some oxadiazole derivatives as novel amide-based inhibitors of soluble epoxide hydrolase. Lett Drug Design Discov. 2014;11:721–30. doi: 10.2174/15701808116661402200055 30.

Zhang J, Li JC, Song JL, Cheng ZQ, Sun JZ, Jiang CS. Synthesis and evaluation of coumarin/1,2,4-oxadiazole hybrids as selective BChE inhibitors with neuroprotective activity. J Asian Nat Prod Res. 2019;21:1090–103. doi: 10.1080/10286020.2018.1492566.

Zhao YH, Abraham MH, Le J, Hersey A, Luscombe CN, Beck G, et al. Rate-limited steps of human oral absorption and QSAR studies. Pharm Res. 2002;19:1446–57. Doi: 10.1023/a:1020444330011.